RSC Advances

PAPER

View Article Online
View Journal | View Issue

Cite this: *RSC Adv.*, 2019, **9**, 429

Amplitude response of conical multiwalled carbon nanotube probes for atomic force microscopy†

Xiao Hu,‡[ab] Hang Wei,‡[ab] Ya Deng,[ab] Xiannian Chi,[ab] Jia Liu,[ab] Junyi Yue,[ab] Zhisheng Peng,[ab] Jinzhong Cai,[ab] Peng Jiang *[a] and Lianfeng Sun *[a]

Received 19th October 2018
Accepted 18th December 2018

DOI: 10.1039/c8ra08683d

rsc.li/rsc-advances

Carbon nanotubes are considered as great candidates for atomic force microscopy (AFM) probes because of their high aspect ratio and outstanding mechanical properties. In this work, we report that a conical AFM probe can be fabricated with arc discharge prepared multiwalled carbon nanotubes (MWCNTs) with an individual MWCNT at the apex by dielectrophoresis. The amplitude–displacement curve of the conical MWCNT probe demonstrates that this structure can remain stable until the force exerted on it increases to 14.0 ± 1.5 nN (nanonewton). Meanwhile, the conical MWCNT probes are able to resolve complex structure with high aspect ratio compared to commercial AFM probes, suggesting great potential for various AFM applications.

Introduction

In the past thirty years, atomic force microscopy (AFM) has emerged as a powerful and versatile tool for the characterization of nanomaterials in nanoscience and nanotechnology.[1–3] The resolution of AFM highly depends on the geometry of the probe, for the obtained image is a convolution of the probe shape with the surface topography. Carbon nanotubes (CNTs) have been proved to be ideal AFM probes for their small dimensions, high aspect ratio and extraordinary mechanical properties.[4,5] Both single-walled carbon nanotubes (SWCNTs) and multiwalled carbon nanotubes (MWCNTs) are able to be used as AFM probes. SWCNTs have a small diameter and well-defined cylindrical graphite shells, while MWCNTs have multiple concentric cylinders with larger lateral stiffness. The cylindrical nature of CNTs makes them reversibly buckle rather than break when axial compression is applied to them. Several effective techniques have been developed to fabricate CNT probes such as optical microscope-based manipulation and scanning electron microscope (SEM)-based manipulation.[6–10] However, direct manipulation is time-consuming and hard to scale up to provide commercially available probes. Since chemical vapor deposition (CVD) was developed as a simple and cheap method to produce carbon nanotubes, both MWCNTs and SWCNTs have been directly grown onto the apex of the catalyst-coated probe.[11,12] This is the most promising method to produce CNT probes in wafer scale, but the length and orientation of carbon nanotube on the apex is hard to control during the growth process. Moreover, the growth of single carbon nanotube on the apex instead of bundles of nanotubes is still a big challenge. Another quick and reproducible technique is utilizing van der Waals interaction between probe and carbon nanotubes to pick up single SWCNT from the substrate during AFM probe imaging.[13] By carefully controlling the scan area, either bundle probes or individual SWCNT probes can be fabricated. However, substrates with vertically aligned SWCNTs are inadequate for wafer scale fabrication CNT probes and this method is not capable of control the length and orientation of CNT as direct growth. On the other hand, the *in situ* attachment of CNT can also be achieved by applying a current flow through a conductive probe and designated MWCNTs. This method is able to control the length and orientation of CNT without any additional process.[14] Dielectrophoresis (DEP) is a technique usually used to manipulate and assemble colloidal particles. Since the method to solubilize carbon nanotubes was developed, separating and arranging CNTs has become possible by using their electronic and physical properties.[15–18] By applying an alternating electric field between electrodes immersed in CNT suspension, CNT probes were fabricated with controlled length and orientation successfully. Since it is rapid and reproducible, DEP is a promising method to fabricate CNT AFM probes.

In this paper, we performed a DEP process in arc-discharged MWCNT suspension to fabricate conical structure onto conductive commercial AFM probe with individual nanotube protruding at its end. Amplitude–displacement curves of these conical probes were measured in tapping mode. The result showed that this structure could remain stable until the force exerted on it increased to 14.0 ± 1.5 nN. The topography

[a]*CAS Key Laboratory of Nanosystem and Hierarchical Fabrication, CAS Center for Excellence in Nanoscience, National Center for Nanoscience and Technology, Beijing 100190, China. E-mail: slf@nanoctr.cn; pjiang@nanoctr.cn*

[b]*University of Chinese Academy of Sciences, Beijing 100049, China*

† Electronic supplementary information (ESI) available. See DOI: 10.1039/c8ra08683d

‡ Xiao Hu and Hang Wei contributed to this work equally.

difference of SWCNT networks scanned by conical probes and commercial AFM probes showed these conical probe are able to resolve complex structure with high aspect ratio and have great potential in AFM imaging.

Experimental

The MWCNTs used in this work were prepared by electric arc discharge method as reported previously.[19] The diameter and length of the MWCNTs are in the range of 5–30 nm and 1–10 μm, respectively. The MWCNT percentage contained in the product was 20–40% and the remainder was graphitized and amorphous carbon nanoparticles. The MWCNT suspension was prepared by dispersing 10 mg MWCNT product in 5 mL ethanol using ultra-sonic bath and then diluted by 20 mL deionized water. The conical CNT probes used in this work were fabricated using a DEP technique. A conductive AFM probe (SCM-PIT, Bruker) with spring constant around 2.8 N m^{-1} was mounted onto a three-dimensional manipulator as the working electrode and a copper ring with a diameter of 2 mm was made as the counter electrode. After a droplet of MWCNT suspension was placed on the copper ring, a function generator was used to apply alternating electric field (10 V at 10 MHz) between AFM probe and copper ring. With an optical microscope mounted on the side of electrodes, the apex of AFM probe and the outline of suspension droplet were placed in the same focal plane of the optical microscope to control the orientation of CNT on the probe. The apex is partially, instead of all, immersed into the suspension. Then the alternative electric field was applied to the electrodes. Withdrawal of the probe resulted in a bundle attached probe. The fabricated probes were annealed at 120 °C in nitrogen for 30 minutes to strengthen the structure on probe apex. The morphology of MWCNT was characterized by transmission electron microscope (TEM, Tecnai G2 F20 U-TWIN) and the morphology of conical probe was characterized by scanning electron microscope (SEM, Hitachi S-4800). The AFM imaging and force calibration were performed on an AFM instrument (Multimode Nanoscope V) using a conductive AFM probe (SCM-PIT, Bruker) with spring constant around 2.8 N m^{-1}. The conductive cantilever had a pyramid-shaped tip with a curvature of the apex around 20 nm. The SWCNT was grown using floating catalytic chemical vapor deposition with 1000 sccm Ar/10 sccm CH_4 at 1100 °C, and deposited on a Si surface with controlled density.

Results and discussion

The key step of fabricating conical CNT probes is the attachment of CNT bundles to the conductive probe. In order to demonstrate this procedure, a DEP process recorded with an optical microscope is shown in Fig. 1. In Fig. 1(a), the apex of the conductive probe is brought into contact with a droplet of MWCNT suspension. Driven by the alternating electric field from the function generator, the product in the suspension aggregate to probe and assemble into a conical structure. As the probe is withdrawn in a controlled manner, the conical CNT probe becomes longer with the continuous growth of conical structure, which is shown in Fig. 1(b). The final step, as shown in Fig. 1(c), is separating of tip and suspension in order to stop the process of DEP, leaving as-fabricated conical CNT probe. In order to control the orientation of the conical CNT probe, the cantilever of the probe and the outline of suspension droplet are both placed in the same focal plane of the optical microscope. In this way, the growth direction of conical structures is guaranteed to be the same path as AFM probe travels.

The morphology of a typical conical CNT probe is shown in Fig. 2(a). MWCNTs, entangled with other forms of carbon, are attached to the side of the pyramidal probe under the guide of electrical force generated by DEP. The body of this conical structure grows from the apex of the probe and extends along the direction of the original tip. An individual MWCNT is straightly protruding from the end, which is shown in Fig. 2(b). In Fig. 2(c), a TEM image shows the high graphitization of MWCNT, which indicates the high quality of the MWCNT. The key to establishing this conical morphology of probe is the pyramidal geometry of the conductive probe. In the DEP process, MWCNTs carry other forms of carbon and attach to the side of the AFM probe tightly owing to the van der Waals interaction. After the root of the structure is formed along the plane of the probe, the subsequent components will continue to grow on it and align as a cone. Previous works have demonstrated that the diameter of the fabricated structure depends on several parameters such as the drawing rate, the electrical field gradient, and the diameter of the probe and the concentration of suspension. In this experiment, the MWCNT suspension was diluted by water to modify the contact between suspension and probe. This improvement makes it possible to control the base of the conical structure by adjusting the immerse depth of probe. The length of the cone can be controlled by regulating the distance traveled in Fig. 1(b). Moreover, both turning off the electric field and withdrawal of the probe at a rate faster than the MWCNT deposition rate will stop the assembly process. By controlling these parameters, probes ranging from 2–15 μm were fabricated. An annealing process is performed to remove the solvent for the stability of probes. Controlling the orientation and length of CNT probe has been proved to be significant for the application in AFM imaging. Apart from the DEP assembly, direct manipulation (under SEM) and CVD *in situ* growth are most widely used in the fabrication of CNT probes. Direction manipulation can realize ideal control of the orientation of CNT using the three-dimensional manipulator and a series of cutting techniques have also been developed to modify the length of CNT probe. However, it is too time-consuming to assemble CNT probes in batches under an SEM. The other method, CVD growth, has been considered as the most efficient technology to fabricate CNT probes, because many CNTs can grow at the same time to realize the assembly. Nevertheless, these probes still suffer from random orientation and length, which needs further improvements in the growth process. Compared to the CVD growth, our DEP process realizes the control of the length and orientation of probe using a three-dimensional manipulator and an optical microscope. Compared to the direct manipulation, it is more convenient to assemble probes in ambient condition than in SEM.

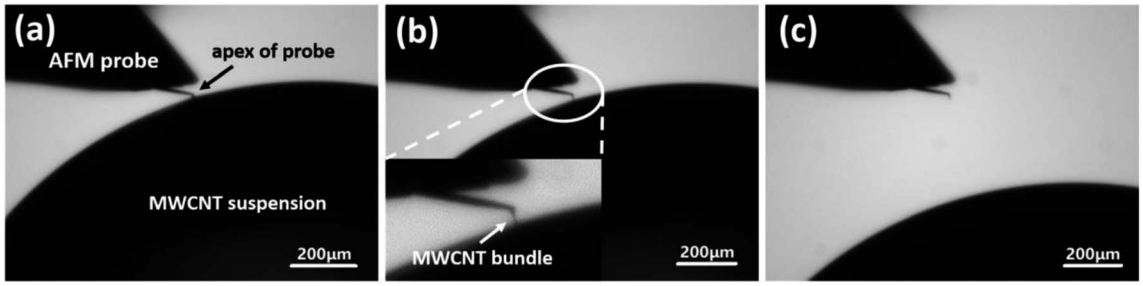

Fig. 1 Optical images of fabrication processes of a conical MWCNT probe by dielectrophoresis. (a) Optical image of the apex of probe immersed into the suspension. After a droplet of MWCNT suspension was put on the copper ring electrode, the apex of the AFM probe and the outline of the droplet are placed in the same focal plane of the optical microscope. Then the apex is immersed into the suspension and an alternating electric field voltage (10 V, 10 MHz) is applied to the probe and copper electrode. (b) Optical image of the apex of probe withdrawn from the suspension. The probe is repeatedly withdrawn from the suspension several times. In the meantime, the growth of MWCNT bundle on the apex can be observed. (c) Optical image of the apex of probe separated with the suspension.

It should be mentioned that the CNT tips have been fabricated using DEP previously.[18] However, there are significant differences between ref. 18 with this work: first, the MWCNTs in this work are prepared by arc discharge,[19] which have the advantage of high degree of graphitization comparing to those MWCNT used in ref. 18 grown by CVD. Second, the MWCNTs tips in this work has a conical structure, which is stable when used as AFM tips. In contrast, the SWCNT or MWCNT tips appeared to be a small bundle with uniform diameter at the tip part in ref. 18. Meanwhile, the AFM tips in this work are also different from those reported in ref. 17: first, ref. 17 used SWCNTs to fabricate AFM probes. In contrast, we use arc discharge grown MWCNT to fabricate AFM probes. Second, the resultant SWCNT tips in ref. 17 are far from ideal, with many bending away from the tip orientation or exhibiting significant curvature near the end. In this work, the probes are straight from the original probe and have ideal geometry with high aspect ratio, as shown in Fig. 2. Third, the probes in ref. 17 are unable to give a recognizable topography unless a stabilization procedure is performed, which usually takes 1–20 minutes to acquire stable image. In contrast, our conical probes are more stable and can give improved image compared to commercial probes without the pre-stabilization process.

Amplitude–displacement curves which record the oscillation amplitude of probe as a function of the displacement of the scanner are important to study the properties of both probes and samples. In order to investigate the motion state of the conical probe under compressive force, the amplitude–displacement curves were measured by ramping a conical CNT probe to a flat portion of a Si substrate. Driven by a piezoelectric actuator, the oscillation amplitude of the cantilever was recorded at its resonance frequency. Fig. 3(a) shows the amplitude–displacement curve of MWCNT probe during approaching to the Si surface. In stage I, the probe is oscillated at its resonant frequency by the piezoelectric actuator. Accompanying with the motion of AFM scanner, the probe is descending towards the substrate and stays at a constant amplitude simultaneously. When the probe is lowered to the position where tip starts to touch the Si surface during its oscillation, stage II begins with the decrease of amplitude. In stage II, the amplitude of probe declines linearly with the displacement of the scanner. As the probe descends lower and lower, a discontinuous change of amplitude is observed at stage III. After the amplitude drops to nearly zero, the oscillation of probe almost ceases, while the scanner continues to bring it down to the surface, as demonstrated in stage IV. In this stage, the probe stays static. However,

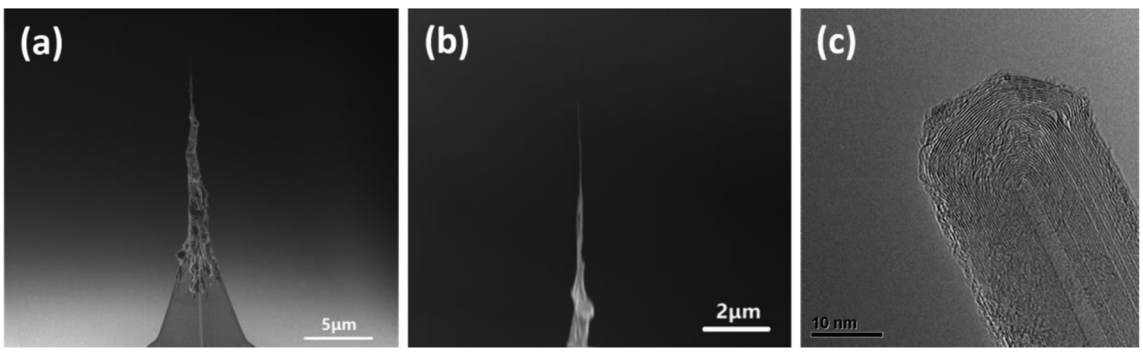

Fig. 2 Characterizations of conical MWCNT probe with SEM and TEM. (a) SEM image of a typical conical MWCNT probe. MWCNTs and other forms carbon (graphitized, amorphous carbon) in the suspension attach to the surface of the AFM probe and form a conical structure along the apex of the original pyramidal tip. The length of the conical structure is around 14 μm. (b) High magnification SEM image showing an individual MWCNT on the end of the tip. The length of the protruding part is around 2.5 μm. (c) TEM image of a typical MWCNT used for fabrication of conical AFM probe. The high graphitization indicates the high quality of the MWCNT and its outer diameter is about 26 nm.

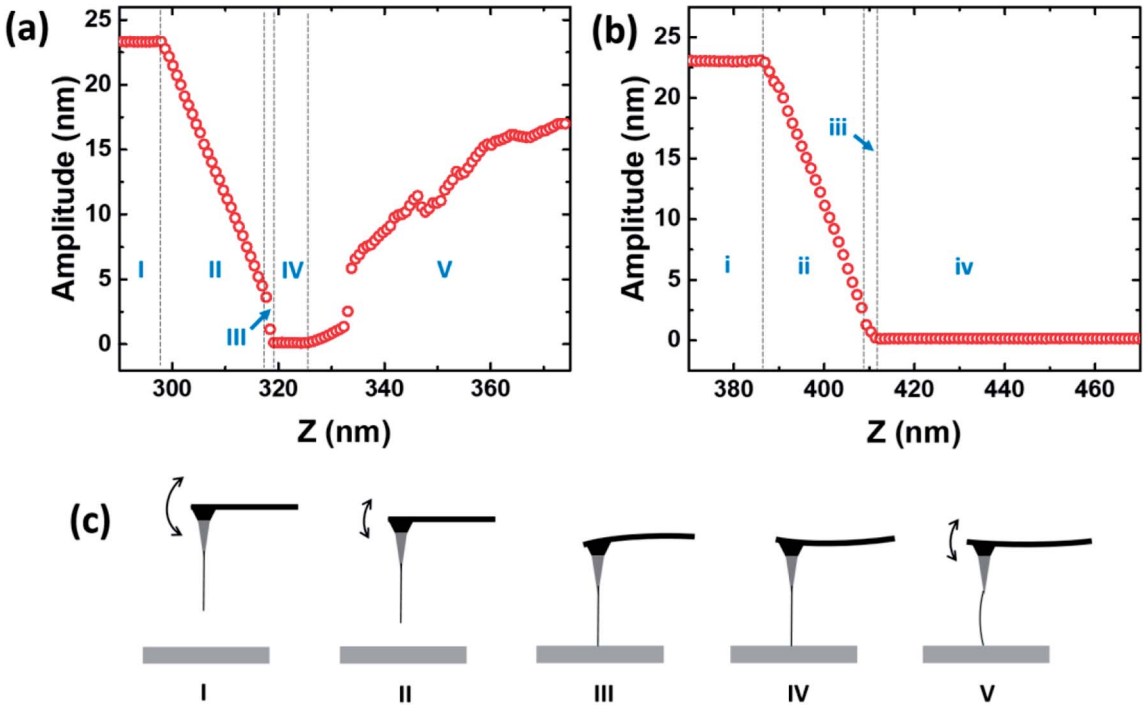

Fig. 3 Amplitude–displacement curve of conical MWCNT probe. (a) Amplitude–displacement curve of conical MWCNT probe. The conical probe is oscillated at its resonant frequency and pushed to a Si substrate. In the meantime, the oscillation amplitude and the displacement of the probe (*Z*) are recorded by AFM controller. I, II, III, IV, V represent different stages of the motion of probe, respectively. (b) Amplitude–displacement curve of commercial AFM probe. i, ii, iii, iv represent different stages of the motion of probe, respectively. (c) Schematic illustration of the motion of the conical probe in different stages: (I) free oscillation. (II) Damped oscillation. (III) Snap to contact. (IV) Bending cantilever without oscillation. (V) Probe resumes oscillating with deformation of MWCNT.

in stage V, an increase of amplitude is observed, which indicates that the probe resumes vibrating.

The proposed motions of the probe in different stages are shown in Fig. 3(b). Due to the damping of the substrate in descending, the tip vibrates with decreasing amplitude, as shown in stage I and II. In stage III, a snap-in event occurs. The probe crashes onto the substrate surface due to the attractive interaction from the substrate. After the apex pressed on the surface in stage IV, the cantilever is bending continually to react to the descending of the probe. In stage V, the pressure from the cantilever is enough to deform the MWCNT structure and the elastic deformation of MWCNT causes the recovery of oscillation. When the deformation becomes larger and larger, the amplitude increases with the displacement of the scanner. This process can be repeated for several times, which indicates the stability of conical structure.

The motion of the AFM probe is related to both attractive and repulsive force during imaging. Previous work has investigated the bistable behavior of AFM probes in amplitude modulated mode.[20] A probe may work on either in attractive regime or repulsive regime. A transition between two oscillation states often causes an unstable image, which depends on the drive amplitude, drive frequency, stiffness of probe and sample. Unlike pyramidal AFM probes, the transition of CNT probes between the attractive region and repulsive region depends on the length, orientation and type of CNT. When the attractive force becomes large enough, the oscillation amplitude of the CNT probe will drop to nearly zero, as known as the snap-in behavior of CNT probe. This behavior is due to the elastic deformation of MWCNT and will affect the feasibility of the CNT probe.[21] The work of Chen *et al.* shows that shorter CNT probes suffer less than longer probes and small-angled CNT probes are harder to snap during imaging.[22] In our results, the snap-in event is observed after an 85% decrease of the original amplitude in stage III.

The mechanical properties of conical CNT probes are revealed after the tip crash into the substrate in stage IV and V. Under the axial compression of scanner during tapping mode, the conical-shaped MWCNT probes show different motions from commercial probes. In stage IV of Fig. 3(a) and S1(a) (ESI†), the amplitude of conical probe stays at nearly zero while the deflection of cantilever is linearly increasing simultaneously. This behavior is same to the amplitude–displacement and deflection–displacement curves of commercial probes, which is shown in the stage iv of Fig. 3 and S1 (ESI†), respectively. The slope of the deflection–displacement curve in stage IV, which is known as "sensitivity", is significant to determine the spring constant of an AFM probe experimentally. According to the displacement in stage IV, the force exerted on the conical probe is evaluated as 14.0 ± 1.5 nN. However, the conical structure is unable to stay stable under the increasing compression of the cantilever. The Euler buckling and the kinking of MWCNT are observed successively in stage V.[23,24] In the forepart of stage V (*Z*: 326 nm–333 nm), the amplitude begins to increase again and

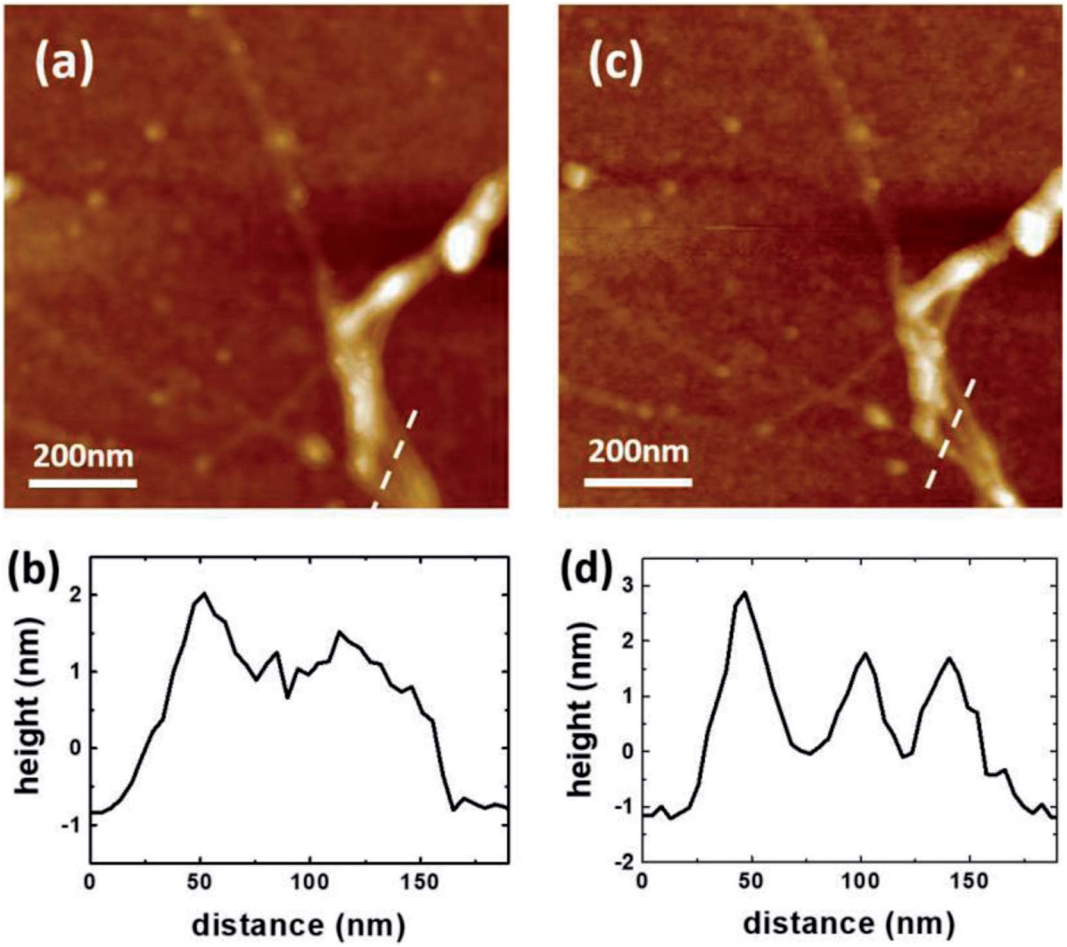

Fig. 4 Imaging comparison between commercial AFM probe and conical MWCNT probe. (a) Topography of complicated single-walled carbon nanotube (SWCNT) networks on a Si substrate scanned by a commercial AFM probe. The height profile along the dashed line is shown in (b). About two bundles of SWCNTs can be identified. (c) Topography of the same SWCNT networks scanned by a conical MWCNT probe. It can be seen that most features of the image are similar to that in (a), indicating the feasibility of our probe for imaging application. What is more interesting is the height profile along the dashed line shown in (d) scanned with the conical MWCNT probe. Three bundles of SWCNTs can be observed clearly. This indicates that conical MWCNT probes are able to resolve complex structure with high aspect ratio.

a nonlinear increase is observed in the deflection of cantilever. This nonlinear behavior of deflection is consistent with Euler buckling as Hsao *et al.* reported in the axial compression of MWCNT.[23] Moreover, the jump of amplitude and deflection in stage V ($Z = 333$ nm in Fig. 3(a) and S1(a)†) is reproducible as shown in Fig. S2 (ESI†). This behavior is consistent with the mechanics of kinking.[23]

The difference between normal AFM probes and MWCNT probes is that MWCNT probes have MWCNT aggregates (graphitized, amorphous carbon and MWCNTs) at the apex. This cause the amplitude response of MWCNT probes is different from normal AFM probes: first, a snap-in event can be observed in the stage III of conical MWCNT probes, which is caused by the elastic deformation of MWCNT, while the amplitude decreases to zero linearly in the stage iii of normal probes, as shown in Fig. 3(b). Second, the amplitude of MWCNT probes stays at zero in the stage IV with the bending of cantilever, which is same to the normal AFM probes in the stage iv. After the force exerted to MWCNT probes is higher than 14.0 ± 1.5 nN, the Euler buckling and kinking of MWCNT can be observed successively. In contrast, normal AFM probes still stays at a zero amplitude with a linear increasing cantilever deflection, as shown in Fig. 3(b) and S1(b) (ESI†), respectively. Comparing the results in ref. 24, the MWCNT aggregates strengthen the stability of MWCNT probes and the conical probes can sustain an axial compression as large as 14.0 ± 1.5 nN without deformation after they crush onto the surface.

In order to demonstrate the imaging capability of the conical probe, SWCNTs grown by CVD were chosen as the test sample. After depositing them on a Si substrate, topography images were acquired in tapping mode by using both commercial AFM probe and conical probe, as shown in Fig. 4. In Fig. 4(a) and (b), the main features of complicated SWCNT networks can be distinguished by the commercial probe, while the conical probe is able to characterize the topography with more details. As illustrated in Fig. 4(c) and (d), two height profiles were extracted from the same position of topography acquired by the commercial probe and conical probe, respectively. In Fig. 4(c), there are two peaks in the height profile, which indicates that the commercial probe distinguished two

SWCNT bundles in the complicated networks. On the other hand, three peaks are observed in the height profile of Fig. 4(d), which is the same position characterized by the conical probe. The radius of both commercial probe and MWCNT conical probe is determined by the method reported previously.[25] As shown in Table S1 (ESI†), the MWCNT probe (42.1 nm) has a smaller radius than that of commercial probe (48.3 nm). Moreover, MWCNT probes are able to resolve complex structures with high aspect ratio. With individual MWCNT on the apex of the conical structure, conical probes can reduce the contact between sample and side of the tip during imaging. Thus an improved topography can be acquired by conical probes. To demonstrate the feasibility and advantage of conical MWCNT probes for AFM imaging, more AFM topography data of SWCNT networks acquired by both conical probes and commercial probes are shown in Fig. S3 (ESI†). It has been reported that the length of CNT attached to an AFM probe is a critical parameter in the stability of the CNT probe.[15] When the length of MWCNT exceeds 1 μm (100 nm for SWCNT), CNT probes are no longer to give reliable image due to thermal vibration. In this work, the total length of the conical structure of probes is in a range of 2 μm to 15 μm. By applying electric shorten method reported before to modify the length of MWCNT at the very end, these probes are capable of giving stable topography of sample in tapping mode AFM.[11] After working for several hours, SEM images of conical probes showed that they remained intact.

Conclusions

In summary, we demonstrate a method to fabricate conical MWCNT probes by using dielectrophoresis and characterize the amplitude response of them under controlled compression. Under the effect of electric field, MWCNTs and other forms carbon coagulate at the apex of the conductive probe to form a conical structure. In order to demonstrate mechanical properties of conical CNT probe, amplitude–displacement curves were measured in the tapping mode. A snap-in event was observed and the cantilever bent after the amplitude dropped to nearly zero, which indicates the conical structure can sustain a fore as large as 14.0 ± 1.5 nN. Conical structures such as carbon nanocone are believed to be promising AFM probes for their high stability.[26] Compared to commercial AFM probes, these conical probes are able to resolve complex structure with high aspect ratio, which makes them have potential for many AFM applications.

Conflicts of interest

There are no conflicts to declare.

Acknowledgements

This work was supported by the Major Nanoprojects of Ministry of Science and Technology of China (Grant No. 2018YFA0208403, 2016YFA0200403), National Natural Science Foundation of China (Grant No. 51472057, 11874129) and Baotou Rare Earth Research and Development Centre (GZR 2018001), Chinese Academy of Sciences (Grant No. XXH13505-03-212).

Notes and references

1 H. J. Butt, B. Cappella and M. Kappl, *Surf. Sci. Rep.*, 2005, **59**, 1–152.
2 R. Garcia and R. Perez, *Surf. Sci. Rep.*, 2002, **47**, 197–301.
3 F. J. Giessibl, *Rev. Mod. Phys.*, 2003, **75**, 949–983.
4 N. R. Wilson and J. V. Macpherson, *Nat. Nanotechnol.*, 2009, **4**, 483–491.
5 R. Zhang, Y. Zhang and F. Wei, *Chem. Soc. Rev.*, 2017, **46**, 3661–3715.
6 H. J. Dai, J. H. Hafner, A. G. Rinzler, D. T. Colbert and R. E. Smalley, *Nature*, 1996, **384**, 147–150.
7 N. de Jonge, Y. Lamy and M. Kaiser, *Nano Lett.*, 2003, **3**, 1621–1624.
8 X. Wei, Q. Chen, L. Peng, R. Cui and Y. Li, *Ultramicroscopy*, 2010, **110**, 182–189.
9 D. S. Ashley, J. S. Cameron, T. G. Christopher, G. S. Joseph, A. L. David and J. S. Andrew, *Nanotechnology*, 2016, **27**, 475708.
10 A. Slattery, C. Shearer, J. Shapter, A. Blanch, J. Quinton and C. Gibson, *Nanomaterials*, 2018, **8**, 807.
11 J. H. Hafner, C. L. Cheung and C. M. Lieber, *J. Am. Chem. Soc.*, 1999, **121**, 9750–9751.
12 Q. Ye, A. M. Cassell, H. B. Liu, K. J. Chao, J. Han and M. Meyyappan, *Nano Lett.*, 2004, **4**, 1301–1308.
13 J. H. Hafner, C. L. Cheung, T. H. Oosterkamp and C. M. Lieber, *J. Phys. Chem. B*, 2001, **105**, 743–746.
14 J. X. Xu, Y. Shingaya, Y. L. Zhao and T. Nakayama, *Appl. Surf. Sci.*, 2015, **335**, 11–16.
15 J. Tang, G. Yang, Q. Zhang, A. Parhat, B. Maynor, J. Liu, L. C. Qin and O. Zhou, *Nano Lett.*, 2005, **5**, 11–14.
16 V. Dremov, V. Fedoseev, P. Fedorov and A. Grebenko, *Rev. Sci. Instrum.*, 2015, **86**, 053703.
17 A. D. Slattery, C. J. Shearer, J. G. Shapter, J. S. Quinton and C. T. Gibson, *Nanomaterials*, 2017, **7**, 346.
18 J. Zhang, J. Tang, G. Yang, Q. Qiu, L.-C. Qin and O. Zhou, *Adv. Mater.*, 2004, **16**, 1219–1222.
19 L. F. Sun, S. S. Xie, W. Liu, W. Y. Zhou, Z. Q. Liu, D. S. Tang, G. Wang and L. X. Qian, *Nature*, 2000, **403**, 384.
20 R. Garcia and A. San Paulo, *Phys. Rev. B: Condens. Matter Mater. Phys.*, 1999, **60**, 4961–4967.
21 E. S. Snow, P. M. Campbell and J. P. Novak, *Appl. Phys. Lett.*, 2002, **80**, 2002–2004.
22 A. N. Jiang, S. Gao, X. L. Wei, X. L. Liang and Q. Chen, *J. Phys. Chem. C*, 2008, **112**, 15631–15636.
23 H. W. Yap, R. S. Lakes and R. W. Carpick, *Nano Lett.*, 2007, **7**, 1149–1154.
24 C. L. Cheung, J. H. Hafner and C. M. Lieber, *Proc. Natl. Acad. Sci. U. S. A.*, 2000, **97**, 3809–3813.
25 Y. Wang and X. Chen, *Ultramicroscopy*, 2007, **107**, 293–298.
26 W. Huang, J. X. Xu and X. Lu, *RSC Adv.*, 2016, **6**, 25541–25548.

